

Interaction of incoherent two-dimensional photorefractive solitons

A. Stepken and F. Kaiser

Institute of Applied Physics, Darmstadt University of Technology, Hochschulstrasse 4a, 64289 Darmstadt, Germany

M. R. Belić

Institute of Physics, P.O. Box 57, 11001 Belgrade, Yugoslavia

W. Królikowski

Laser Physics Centre, Australian National University, Canberra, Australian Capital Territory 0200, Australia

(Received 8 June 1998)

Numerical and experimental investigation of the interaction between incoherent spatial photorefractive solitons is performed. It is found that the interaction between two-dimensional solitons is different from the interaction between one-dimensional solitons. Whereas one-dimensional incoherent solitons display only attraction, two-dimensional solitons can display repulsion as well as attraction. [S1063-651X(98)50910-5]

PACS number(s): 42.65.Tg, 42.65.Hw

Much attention is focused on the recently discovered photorefractive (PR) spatial screening solitons [1]. They emerge when laser beams of appropriate wavelength, intensity, and shape are launched into a PR crystal, and a dc electric field is applied in the lateral direction, to induce self-focusing of beams through PR screening [2]. Their unique properties make them promising for all optical applications [3,4]. Soliton-induced guiding or switching devices make use of two or more solitons, so that the study of their interaction behavior is of central interest.

As is known [5], coherent solitons in one transverse dimension (1D) and in two transverse dimensions (2D) display both attraction and repulsion, depending on the phase difference between them. The interference of optical fields causes an increase or decrease in the refractive index, and attraction or repulsion between solitons, respectively. In collisions, they can exchange energy and thus are able to annihilate each other, or to give birth to new solitons [6]. The coherent solitons tend to build diffraction gratings, and an additional energy transfer process, due to two-wave mixing, can play an important role and can make the control of solitons difficult.

Incoherent solitons are more manageable, but it was believed that they can only attract [7,8]. Recently it has been demonstrated that incoherent spatial solitons can display both attraction and repulsion [9]. If two solitons propagating parallel are launched in the plane parallel to the direction of the applied field, they exhibit the so-called anomalous interaction behavior. They attract if the initial separation is of the order of the beam diameter, and they repel otherwise.

Based on these observations, we demonstrate that the attraction and the repulsion of 2D incoherent solitons is determined by their positions in the transverse plane and the distance between them. Depending on the initial conditions, we see both numerically and experimentally interesting propagation effects. When the two solitons are launched in the plane perpendicular to the direction of the applied field (and the diffusion field is small), they only attract and fuse, staying in the plane. If the launching plane is at an angle to the applied field, the solitons rotate or oscillate, still attracting or repelling each other, depending on the initial separation and po-

sition. When the effect of charge carrier diffusion is taken into account, the solitons drift in the direction of the applied field [10]. However, this effect depends on the number of solitons and on their position. When the drift of solitons, due to nonparallel launching, is taken into account, then the “dynamics” in the transverse plane becomes complicated. Solitons spiral about each other, oscillate, fuse and defuse, drift, and produce other “dancing acts.”

With such premises, we furnish experimental and numerical details and provide an explanation for the observed phenomena. Experiments [6] are performed on a crystal of strontium barium niobite (6-mm cube), doped with Cr. Incident beams are derived from an argon ion laser (514.5 nm). Two beams with $w_0 = 15 \mu\text{m}$ full width at half maximum (FWHM) spot size are launched onto the a face of the crystal. They are polarized along the c axis to make use of the dominant r_{33} electro-optic coefficient, which was measured to be 180 pm/V. A voltage of 2 kV is applied perpendicularly to the propagation direction along the c axis. The distance between beams, their position and launching directions in the transverse plane, as well as the degree of their coherence, can all be adjusted. One of the beams was phase modulated by a piezo-electric transducer to achieve incoherence. A white light source was used to control the value of the saturation intensity. The input and output light intensity distributions were recorded with a charge-coupled device (CCD) camera, and the ratio between soliton intensity and saturation intensity is chosen to be around 2.

In numerical simulations the input face is denoted as the (x,y) plane, and the direction of the external field is taken as the x axis. The beams are assumed to propagate roughly in the positive z direction. Initially, Gaussian beams [11] are launched into the crystal.

The model for the crystal-light interaction is adopted from Ref. [2], with some important changes, and extended to two transverse dimensions. First, we include drift terms in the propagation equations. This must be done as soon as one has more than one beam to contend with, which need not propagate in the same direction. Each beam defines its own paraxial propagation axis, and the slowly varying envelope

wave equation for each of the beams must be transformed to the common (x, y, z) coordinate system, which is attached to the crystal. Second, to model the corresponding response of the material to the presence of the propagating light beams, we introduce the potential of the 2D field distribution $E_{sc} = -\nabla\phi$, where the ∇ operator acts in the transverse plane. Third, we provide for the effects of the charge carrier diffusion, which causes the bending of beams [10]. Fourth, the soliton propagation equations are augmented by a time dependent equation for the development of the screening electrostatic potential. This allows for the slow temporal changes of solitons and the capture of various dynamical effects, such as the development of dynamical lenses in the transient regime of waveguide formation [12].

Propagation equations for the two spatial solitons in the paraxial approximation are of the form

$$\begin{aligned} \partial_z A_1 + \alpha A_1 + \beta(\theta_1^x \partial_x + \theta_1^y \partial_y) A_1 - i(\partial_x^2 + \partial_y^2) A_1 / 2 \\ = i\gamma \partial_x \phi A_1, \end{aligned} \quad (1a)$$

$$\begin{aligned} \partial_z A_2 + \alpha A_2 + \beta(\theta_2^x \partial_x + \theta_2^y \partial_y) A_2 - i(\partial_x^2 + \partial_y^2) A_2 / 2 \\ = i\gamma \partial_x \phi A_2, \end{aligned} \quad (1b)$$

where α is the linear absorption over the diffraction length $l_D = kn_e x_0^2$ (k is the wave number, n_e is the extraordinary index of refraction, and x_0 is the transverse scaling length, typically a beam spot size), $\beta = x_0 / l_D$, and θ specifies the launching angles of the beam. After a propagation of l_D , a beam launched at the origin of the transverse plane will be θ^x (in units of x_0) away from the x axis, and θ^y (again in units of x_0) away from the y axis. $\gamma = k^2 n_e^2 x_0^2 r_{33}$ is the coupling constant and ϕ is the electrostatic potential inside the crystal. Since the screening spatial solitons are observed only when an external electric field is applied, we write $\phi = \phi - E_0 x$, and deal only with the potential $\tilde{\phi}$ induced by the light. The incorporation of boundary conditions is then easy. The temporal equation for the space-charge field is similar to the one derived in Ref. [13], written here for $\tilde{\phi}$,

$$\begin{aligned} \tau \partial_t (\nabla^2 \tilde{\phi}) + \nabla^2 \tilde{\phi} + \nabla \ln(1+I) \cdot \nabla \tilde{\phi} = E_0 \partial_x \ln(1+I) \\ + (k_B T / e) [\nabla^2 \ln(1+I) + (\nabla \ln(1+I))^2], \end{aligned} \quad (2)$$

where τ is the intensity-dependent relaxation time of the crystal, I is the total intensity (measured in units of the saturation intensity), and the operator ∇ acts only on the transverse coordinates x and y . The last term on the right-hand side of Eq. (2) is the diffusion field of the crystal. It can be controlled, for example, by adjusting the temperature T . e is the charge of the dominant carriers. The values of all parameters are chosen consistently with the experimental values.

Numerical integration of Eqs. (1) and (2) is accomplished by a modified spectral split-step method [11], which treats propagating beams separately from the temporal evolution of $\tilde{\phi}$, which is achieved by the Crank-Nicholson method. Thanks to the adiabatic separation of the fast optical from the slow crystal processes, the spatial propagation loop can be separated from and nested within the temporal integration

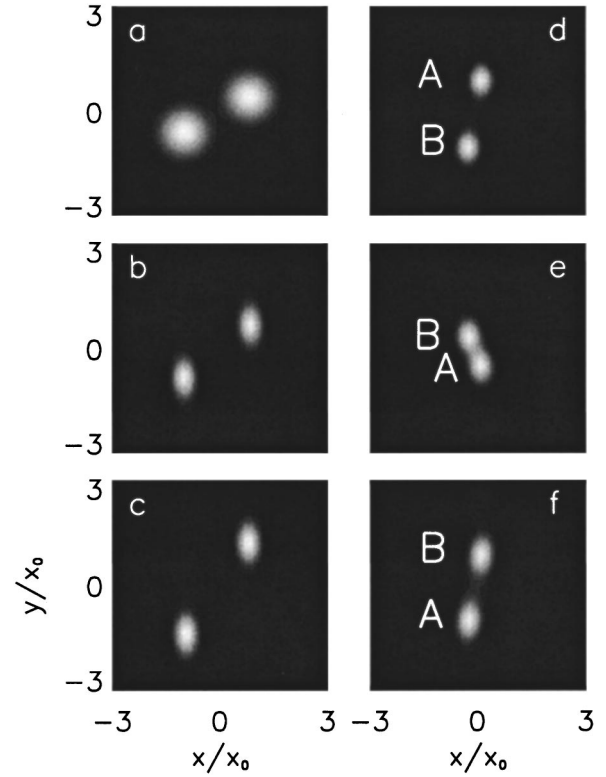


FIG. 1. Interaction of an incoherent pair of spatial solitons; numerical simulation. (a)–(c) Repulsion and rotation of solitons: (a) initial distribution, (b) after 6-mm propagation, (c) after 12-mm propagation. (d)–(f) Spiraling of attracting solitons, injected along the y axis (initial distribution not shown; distance $32 \mu\text{m}$): (d) after 2.4-mm propagation, (e) after 9.6-mm propagation, (f) after 13.2-mm propagation.

loop. In this Rapid Communication we only present steady-state results without damping ($\alpha = 0$).

Figure 1 depicts repulsion and rotation of two incoherent spatial PR solitons. Solitons are launched parallel to each other and at a distance ($31 \mu\text{m}$) that results in repulsion. If they were injected more closely, they would attract. Initially, solitons repel and rotate, until they reach the y axis. Afterwards (not shown) they oscillate about the y axis and attract. Solitons launched close to the y axis always attract. Solitons launched close to the x axis can both repel and attract, depending on the initial separation. The spiraling solitons are shot at the position where they are attracting, and in nonparallel directions (the angular separation is 2.6×10^{-3} rad), so as to boost their angular momentum to overcome an attractive barrier along the y axis and a repulsive barrier along the x axis, and remain bounded. This requires some precise shooting. A similar behavior has been found experimentally in Ref. [8].

Figure 2 offers an explanation for the observed repulsion of solitons. It shows the space-charge field distribution of two solitons situated along the x axis, in one case lying close to each other and in the other case well separated. The distribution of the space-charge field mirrors the change in the refractive index. Thus, the regions where the distribution is below the background level of the applied field signify focusing or attraction, and the regions where the distribution is above the background level signify defocusing or repulsion.

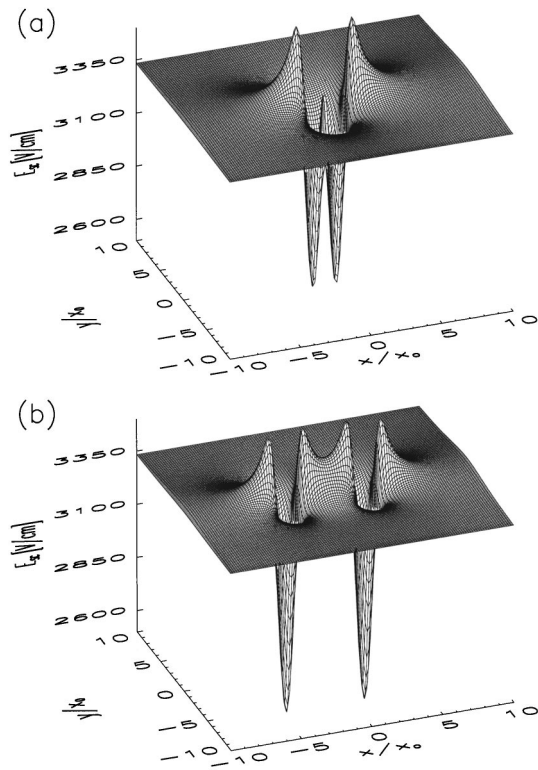


FIG. 2. Transverse distribution of the space-charge field for two solitons situated along the x axis: (a) attracting solitons, (b) repelling solitons.

In the case where they are close enough, the solitons fuse. However, if they are far enough away, then repulsive shoulders appear, and the solitons fly apart. Note that along the y axis only attraction is possible. Repulsive forces are induced along the direction of the external field, which also causes the squeezing of solitons along the x axis. Solitons become elliptical in shape, which is also experimentally observed [13]. If, however, more elongated beams are launched into the crystal, and their intensity is insufficient for stable soliton formation, then they disintegrate fast. Such effects cannot be observed for 1D spatial solitons.

All of our numerical findings are corroborated by our experimental results. Figure 3 presents a comparison for the case of oscillating solitons. In the experiment, two solitons were injected along the y axis such that their individual trajectories would not intersect. During propagation, however, the mutual attraction of beams leads to the crossing of their paths, the exchange of positions, and apparent oscillations around the equilibrium point. The identities of the solitons at the exit plane were determined by blocking one of the input beams. Owing to the slow time scale of the photorefractive process, the refractive index structure induced in the crystal by both beams persisted for some time, thus allowing the remaining soliton to propagate as if the interaction was still present. Exactly the same behavior is found numerically. It is noted experimentally, as well as numerically, that solitons injected parallel off y axis tend to oscillate about the axis, rather than to spiral.

Also, strong bending of solitons is observed experimentally, owing to the influence of the diffusion field. Individual solitons bend differently from the soliton pairs. However, the bending of the “center of mass” of two solitons is similar to

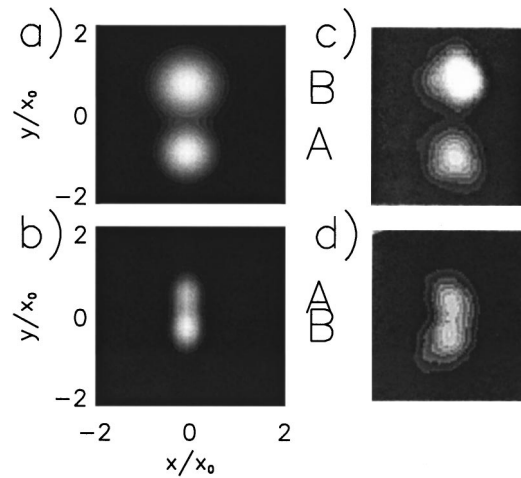


FIG. 3. Numerical (a), (b) and experimental (c), (d) results indicating an oscillation of solitons along the y axis: (a) and (c) are initial distributions; (b) and (d) are distributions after 6-mm propagation.

the bending of one soliton, except for some possible wobbling of the center, due to energy exchange between solitons. These effects are seen in numerical simulation as well. Figure 4 displays the bending of an individual soliton, and the bending of an interacting soliton pair. Approximately, the bending is additive to the “motion” of solitons without diffusion field effects. The direction of bending depends on the sign of the charge carriers.

To conclude, we have investigated both experimentally and numerically the interaction of 2D spatial PR incoherent solitons. It is found that they can both attract and repel, un-

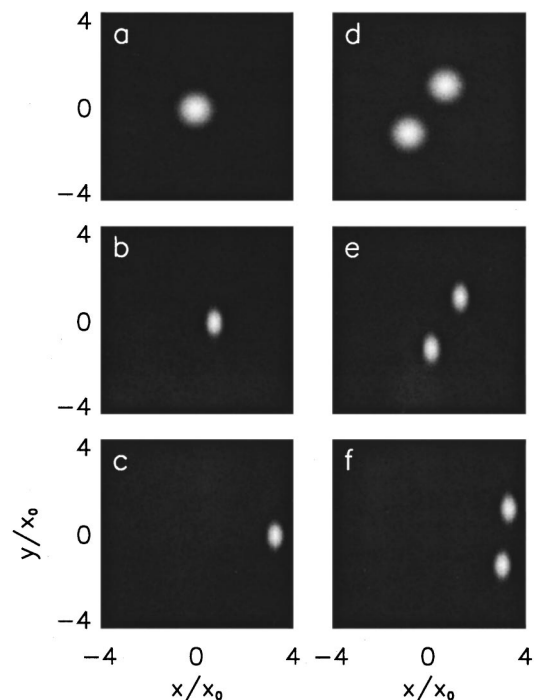


FIG. 4. Soliton bending, owing to the diffusion field. (a)–(c) One spatial soliton, launched along the z axis. (a) Initial distribution, (b) after 6-mm propagation, (c) after 12-mm propagation. (d)–(f), Two bending solitons after the same distances.

like 1D spatial solitons. It is found that they can spiral about each other, but preferably they oscillate about the y axis. Repulsion of solitons is induced along the x axis, that is, in the direction of the external electric field. In addition to repelling, the solitons drift in the direction of the external field, once the diffusion field is accounted for. The drift of individual solitons is different from the drift of two interacting solitons.

It would be interesting to construct a dynamical theory of interacting incoherent 2D solitons, considering them as quasiparticles. Such a theory cannot be a pure mechanical theory of “orbiting” and “repelling” solitons, as electrical effects are playing a prominent role. It cannot be a pure electrome-

chanical theory, as light and PR effects play an important role. Another interesting extension would be to consider the interaction of more than two solitons, and the types of structures they could build in the transverse plane. It is conceivable that the questions of the stability of transverse patterns, as well as the appearance of defects (“birth and death” of solitons) would come to the fore.

The research in Darmstadt was supported within the SFB 185 of the DFG. Research at the Institute of Physics was supported by Project No. 01M07 of the Ministry of Science and Technology of the Republic of Serbia. We would like to thank C. Denz for assistance with experiments and O. Sandfuchs for interesting discussions.

-
- [1] M. Segev, B. Crosignani, A. Yariv, and B. Fischer, *Phys. Rev. Lett.* **68**, 923 (1992); G. Duree, J. L. Shultz, G. Salamo, M. Segev, A. Yariv, B. Crosignani, P. DiPorto, E. Sharp, and R. Neurgaonkar, *ibid.* **71**, 533 (1993); M. Shih, M. Segev, G. C. Valley, G. Salamo, B. Crosignani, and P. DiPorto, *Electron. Lett.* **31**, 826 (1995); M. D. Iturbe Castillo, P. A. Márquez Aguilar, J. J. Sánchez-Mondragón, S. Stepanov, V. Vysloukh, *Appl. Phys. Lett.* **64**, 408 (1994).
- [2] D. N. Christodoulides and M. J. Carvalho, *J. Opt. Soc. Am. B* **12**, 1628 (1995).
- [3] A. W. Snyder and A. P. Sheppard, *Opt. Lett.* **18**, 482 (1993).
- [4] M. Chauvet, S. A. Hawkins, G. J. Salamo, M. Segev, D. F. Bliss, and G. Bryant, *Appl. Phys. Lett.* **70**, 2499 (1997).
- [5] H. Meng, G. Salamo, M. Shih, and M. Segev, *Opt. Lett.* **22**, 448 (1997).
- [6] W. Krolikowski and S. A. Holmstrom, *Opt. Lett.* **22**, 369 (1997); W. Krolikowski, B. Luther-Davies, C. Denz, and T. Tschudi, *ibid.* **23**, 97 (1998).
- [7] M. Shih and M. Segev, *Opt. Lett.* **21**, 1538 (1996).
- [8] M. Shih, M. Segev, and G. Salamo, *Phys. Rev. Lett.* **78**, 2551 (1997).
- [9] W. Krolikowski, M. Saffman, B. Luther-Davies, and C. Denz, *Phys. Rev. Lett.* **80**, 3240 (1998).
- [10] M. I. Carvalho, S. R. Singh, and D. N. Christodoulides, *Opt. Commun.* **120**, 311 (1995).
- [11] M. Belić, J. Leonardy, D. Timotijević, and F. Kaiser, *J. Opt. Soc. Am. B* **12**, 1602 (1995).
- [12] C. M. Gómez Sarabia, P. A. Márquez Aguilar, J. J. Sánchez Mondragón, S. Stepanov, and V. Vysloukh, *J. Opt. Soc. Am. B* **13**, 2767 (1996).
- [13] A. A. Zozulya and D. Z. Anderson, *Phys. Rev. A* **51**, 1520 (1995); A. A. Zozulya, D. Z. Anderson, A. V. Mamaev, and M. Saffman, *ibid.* **57**, 522 (1998).